Author Manuscript

Author Manuscript

Author Manuscript

Author Manuscript

HHS Public Access

Author manuscript

Oncogene. Author manuscript; available in PMC 2025 January 06.

Published in final edited form as:

Oncogene. 2024 June ; 43(27): 2092–2103. doi:10.1038/s41388-024-03064-7.

AR Loss in Prostate Cancer Stroma Mediated by NF-κB and p38-MAPK Signaling Disrupts Stromal Morphogen Production

Tahsin Shekha[1], **Neha S Sane**[2], **Cernyar Brent**[2], **Jiang Linan**[3], **Zohar Yitshak**[3,4], **Benjamin R Lee**[4,5], **Cindy K Miranti**[1,2,4]

[1]Cancer Biology Graduate Interdisciplinary Program, University of Arizona, Tucson, AZ

[2]Department of Cellular and Molecular Medicine, University of Arizona, Tucson, AZ

[3]Department of Aerospace and Mechanical Engineering,University of Arizona, Tucson, AZ

[4]University of Arizona Cancer Center, University of Arizona, Tucson, AZ

[5]Department of Urology, University of Arizona, Tucson, AZ

Abstract

Androgen Receptor (AR) activity in prostate stroma is required to maintain prostate homeostasis. This is mediated through androgen-dependent induction and secretion of morphogenic factors that drive epithelial cell differentiation. However, stromal AR expression is lost in aggressive prostate cancer. The mechanisms leading to stromal AR loss and morphogen production are unknown. We identified TGFβ1 and TNFα as tumor-secreted factors capable of suppressing *AR* mRNA and protein expression in prostate stromal fibroblasts. Pharmacological and RNAi approaches identified NF-κB as the major signaling pathway involved in suppressing AR expression by TNFα. In addition, p38α- and p38δ-MAPK were identified as suppressors of AR expression independent of TNFα. Two regions of the *AR* promoter were responsible for AR suppression through TNFα. FGF10 and Wnt16 were identified as androgen-induced morphogens, whose expression was lost upon TNFα treatment and enhanced upon p38-MAPK inhibition. Wnt16, through non-canonical Jnk signaling, was required for prostate basal epithelial cell survival. These findings indicate that stromal AR loss is mediated by secreted factors within the TME. We identified TNFα/TGFβ as two possible factors, with TNFα mediating its effects through NF-κB or p38-MAPK to suppress *AR* mRNA transcription. This leads to loss of androgen-regulated stromal morphogens necessary to maintain normal epithelial homeostasis.

Corresponding Author: Cindy K Miranti, PhD, University of Arizona Cancer Center, 1515 N Campbell Ave, Tucson, AZ 85724, cmiranti@arizona.edu.

AUTHOR CONTRIBUTIONS

ST was responsible for designing, carrying out, and interpreting the experiments, as well as the primary writer of the manuscript. NSS and BC designed and carried out experiments and helped edit the manuscript. LJ and YZ assisted with interpretation of data and editing the manuscript. BRL contributed patient tissues and helped with manuscript editing. CM directed the project, assisted in data interpretation, did manuscript writing and editing, and is the contributing author.

HUMAN SUBJECTS

Human tissues used in these studies were deidentified and obtained through the University of Arizona Cancer Center Tissue Biorepository (TACMSR). An approved IRB protocol is used by the Biorepository for the collection of tissues which requires informed consent from all subjects.

Competing Interests

The authors declare they have no competing financial interests.

Author Manuscript Author Manuscript Author Manuscript Author Manuscript

Keywords

Androgen Receptor expression; prostate cancer; stromal fibroblasts; tumor microenvironment; signal transduction; transcriptional regulation; development; differentiation

INTRODUCTION

The normal human prostate gland is arranged in a series of ducts lined with secretory luminal epithelial cells sitting atop basal epithelial cells attached to a basement membrane. The epithelial ducts are embedded in a fibromuscular stroma consisting of fibroblasts and smooth muscle cells. Elegant tissue recombination and mouse genetic studies determined that AR expression in the stroma, but not in the luminal epithelial cells, is required for ductal luminal cell development and that formation of luminal cell-lined ducts is driven by stroma-derived, androgen-regulated paracrine-acting morphogens [1–11]. However, the full details on the androgen-induced paracrine stroma factors that drive luminal cell differentiation have yet to be clearly delineated. Initially, FGF10 and FGF7 (aka KGF) were proposed to be secreted by the stroma in response to androgen, although the results surrounding KGF remain controversial [2, 4, 12–20]. When added exogenously to isolated basal epithelial cells in tissue culture, either FGF10 or FGF7 can induce luminal cell differentiation [8, 16, 21–24]. It remains unclear whether these are the only androgen-induced morphogens.

Prostate cancer, which arises from the epithelial compartment, is dependent on androgens and intrinsic AR activity for their growth and survival. However, AR expression in the surrounding cancer stroma is reduced or absent in prostate cancers [25–30], and positively correlates with disease aggressiveness and poor outcome. Androgen deprivation therapy (ADT), which is the standard of care for advanced prostate cancer, also leads to loss of stromal AR function [6]. However, it is not known how AR is lost from the stroma or its consequence on stromal androgen signaling. Given stromal AR is required to maintain normal prostate homeostasis, its loss may contribute to cancer progression. The ability of tumor cells to convert underlying stromal cells into cancer-associated fibroblasts (CAFs) and the dependency of the tumor on CAFs is well documented [31–37]. Whether stromal AR loss is a consequence of CAF conversion is unknown.

The mechanisms that maintain AR levels are highly complex with control exerted by several pathways in a cell-, tissue-, and developmental stage-specific manner. Most studies on *AR* gene regulation were conducted primarily in tumor cells. The human *AR* promoter lacks a classical TATA-box and contains two initiation sites flanked by GC-rich Sp1 binding sites [38–40]. Numerous transcription factors have been mapped to the *AR* promoter [41]. Some reportedly enhance *AR* mRNA expression, such as Myc [42, 43], CREB [44], FOXO3a [45], Twist1 [46], Smad2/3 [47], Wnt/LEF-1 [48], Zeb1 [49], and GATA2 [50, 51], while others suppress *AR* transcription, such as p53 [52] and E2F1 [53, 54]. Two other regulators of *AR* mRNA expression, NF-κB and AR protein itself have been reported to act as both suppressors and activators depending on the context and cell type. Two AR binding sites are located within the second exon and coding region of the *AR* gene, where depending on the androgen response, can enhance or suppress *AR* gene transcription [43, 55, 56]. Several

Author Manuscript Author Manuscript Author Manuscript Author Manuscript

NF-κB binding sites that enhance *AR* mRNA expression have been mapped on the human [57] and rat [58–60] *AR* gene promoters; however, these sites are not conserved between the species. One upstream NF-κB site in the rat [59] and a binding site in the 5'-UTR of the human *AR* gene reportedly repress AR expression [61, 62]. A caveat of all the human *AR* promoter studies is that they were conducted in metastatic prostate cancer cell lines, primarily LNCaP, which may not completely reflect how *AR* transcription is controlled in normal cells. One exception, ZEB1 binding to the human *AR* promoter was conducted in foreskin fibroblasts [49]. On the other hand, the rat studies were conducted in normal Sertoli or liver cells [58–60].

These studies highlight the varied ways in which *AR* gene transcription can be regulated and highlight the need to better understand specific mechanisms under specific responses in the relevant cell types. These studies also highlight the fact that the mechanisms driving *AR* gene expression in normal prostate stroma are unknown. In this study, we investigated how TNFα, secreted from tumor cells, induces signal transduction pathways that suppress transcriptional regulation of the *AR* gene in human prostate fibroblasts and the consequences on stromal fibroblast morphogens.

MATERIALS AND METHODS

Cell culture.

Benign human prostate stromal cells (BHPrS1), immortalized with hTert, were obtained from Simon Hayward [9]. C4–2 and 22Rv1 cells were obtained from ATCC and grown in RPMI (Gibco) with 10% fetal bovine serum (FBS) and 1% penicillin-streptomycin at 37C in a humidified atmosphere containing 5% CO_2. Three deidentified primary prostate punch biopsies from normal human patient tissue were obtained through our tissue biorepository using an approved IRB protocol. These biopsies were used to isolate stromal fibroblasts. Cells were grown and cultured in the same medium as BHP cells. HPV-immortalized human prostate basal epithelial cells were cultured in KSFM medium supplemented with EGF and BPE as previously described [63]. All cells were routinely tested for Mycoplasma contamination every six months using MycoAlert Mycoplasma Detection Kit (Lonza). Cell lines were validated annually by STR.

Reagents.

Inhibitors BAY-11–7082 (cat S2913), Caffeic Acid Phenethyl Ester (CAPE) (cat S7414), and Takinib (cat s8663) were purchased from Selleck chemicals. 5Z-7-Oxozeaenol (cat O9890) was purchased from Millipore sigma. Pan p38 and Jnk inhibitors, BIRB796, SB202190, AS601245, and SP600125 were purchased from Cayman chemical company.

Cytokine array.

Equal amounts of protein, 100μg, from C4–2 and 22RV1 cells were incubated with a human cytokine antibody array C2000 (Ray Biotech Inc) according to the manufacturer's protocol. Array membranes were incubated with a 1:10 dilution of cell lysate for 2 hours. The array membrane was washed, incubated with a biotin-conjugated anti-cytokine mix for 2 hours, washed again, and developed for 2 hours with biotinylated streptavidin. The membrane

Author Manuscript Author Manuscript Author Manuscript Author Manuscript

signals were captured by scanning and analyzed with the Ray Biotech Analysis tool. Signals were normalized relative to internal positive and negative controls included on the array. Signal intensity was used to rank high, medium high, and medium expression levels relative to the controls.

Conditioned medium assay.

22Rv1 tumor cells were cultured for 7 days in RPMI with 10% FBS and medium was collected (conditioned media). BHPrS1 or a primary human prostate stromal culture were starved 24 h, then treated with conditioned medium from 22Rv1 cells for 24 h. Cell lysates were assessed by immunoblotting.

Cell survival assay.

PrECs were plated at 50% confluency into 24 well tissue culture plates in KSFM with supplements. Cells were then starved in KSFM without supplements for 24h, then treated with different concentrations of Jnk inhibitors for 2–24h in the absence or presence of 0.2–0.8μg/ml Wnt16. Cells were fixed in crystal violet, imaged, and quantified in Synergy2 plate reader.

Immunoblotting.

Cells are lysed in 1X RIPA from Cell Signaling Technology supplemented with a 1:100 Protease/Phosphatase inhibitor cocktail (A32961 Thermo scientific). Protein concentrations were determined using the Pierce™ BCA Protein Assay Kit (23225 Thermo scientific) and 30μg of protein was resolved by electrophoresis on 10% SDS-PAGE. Proteins were transferred onto a PVDF membrane and blocked with 5% BSA in TBST buffer (0.01 M Tris-Cl, 0.15 M NaCl, 0.5% Tween-20, pH 8.0) at room temperature for 1h. The membrane was incubated with indicated antibodies (Supplementary Table S1) overnight at 4C or 3h at room temperature in 5% BSA/TBST followed by a LI-COR secondary antibody for 1h at room temperature. The signal was detected using a LI-COR Odyssey Infrared Imaging System. Alternatively, HRP-secondary antibodies followed by ECL imaging on Genesys system was used.

Immunofluorescence.

Cell lines grown on coverslips were exposed exogenously to 30ng/ml TNFα (R & D) or 10ng/ml TGFβ1 (Tonbo bioscience) for 24h. The cells were fixed for 10 minutes in 4% paraformaldehyde, then permeabilized for 5 minutes in 0.5% Triton-X in PBS and blocked for 1h in 4% BSA in PBS at room temperature. Fixed cells were washed three times with PBS before every step. The indicated primary antibodies (Supplementary Table S1) were diluted in 1% BSA in PBS, while secondary fluorescent antibodies were diluted in PBS. Both were incubated at room temperature for 1h.

Quantitative real-time PCR.

Total RNA was isolated using the RNeasy Plus Kit (Qiagen). RNA (1μg) was employed for first-strand cDNA synthesis using qScript cDNA Super Mix (Quant Bio). The resulting cDNA (30ng) was used as templates for qRT-PCR to analyze mRNA expression using Apex

Author Manuscript Author Manuscript Author Manuscript Author Manuscript

SYBR® Green PCR Master Mix (Genesee Scientific) with primers (Integrated DNA) for *AR*, *FGF10*, *WNT16*, and *KGF* (Supplementary Table S2). Data were normalized to 18S or GAPDH.

siRNA transfection.

Custom siRNA to knockdown Tak1, p38α, and p38δ (Supplementary Table S3) was purchased from Horizon, Inc. BLAST analysis showed no homology of the siRNA sequences to any other sequences in the Human Genome Database. 30nM siRNAs were transfected using Lipofectamine™ RNAiMAX (Thermo Fisher Scientific) according to Horizon protocol in six well plates. A control siRNA pool from Horizon served as a control.

Tet-inducible shRNA.

Doxycycline-inducible shRNA targeting RelA was generated as previously described [19]. Fwd 5'-CTA GCA TGG ATT CAT TAC AGC TTA ATT −3' and Rev 5'-AAT TCA AAA AAT GGA TTC ATT ACA GCT −3' oligos were purchased from IDT. Sense and antisense oligos was annealed and ligated into pLKO-Puro EZTetON lenti-viral vector using Nhe and EcoR1 sites, creating pLKO-EZTetONshRelA [24]. The integrity of the plasmids was verified by sequencing (Eton Biosciences). Lentivirus was packaged in HEK293 cells using packaging plasmids pMD2 and psPAX2 (Addgene) and virus collected 24h later. Virus was used to infect BHPrS1 cells and pools were selected and maintained with 2μg/ml puromycin. Doxycycline (Millipore) at 200 ng/ml was determined to be the optimal dose to inhibit expression within 48h and was used for subsequent assays.

Luciferase assays.

Wildtype *AR* promoter sequence, spanning −1040 to +499, was subcloned into the Nano luciferase reporter vector pNL3.2 [NlucP/minP] (cat N1041; Promega) using the KpnI and BglII (Gene Universal). *AR* promoter deletions were created by Gene Universal. Firefly luciferase reporter driven by the cytomegalovirus (CMV) promoter, pGL4.53[luc2/PGK (cat N1610; Promega), served as the internal control for signal normalization. A non-promoter luciferase reporter was used as a negative control for basal activity of the dual-reporter vector. The constructs were confirmed by DNA sequencing (Eton Biosciences).

BHPrS1 cells were cultured at a density of 2×10^4 cells/well in 96-well culture plates and co-transfected with plasmid reporter DNA either empty, wild type, or mutant *AR* (1 μg PNl-Nano) luciferase construct, along with Firefly luciferase (0.1 μg pGL4.53) for 48h using Fugene (Promega). The activities of Nano and Firefly were determined using the Nano Glo Dual Luciferase Assay Kit (Promega). The luminescence was measured using a Synergy 2 plate reader. The Nano signal was normalized to Firefly.

ChIP assays.

Formalin-crossed chromatin was isolated from BHPrS1 cells treated with or without 30ng/ml TNFα and digested with micrococcal nuclease using Cell Signaling Technology SimpleChIP Enzymatic Chromatin IP Kit. Total nuclear NF-κB and phosphorylated CREB1/ATF1 were immunoprecipitated using ChIP validated antibodies, i.e., P-CREB/ATF1 (9198) and NF-κB (8242) from Cell Signaling Technology. Precipitated chromatin crosslinking was

Author Manuscript Author Manuscript Author Manuscript Author Manuscript

reversed, purified, and used for qPCR using Apex SYBR® Green PCR Master Mix (Genesee Scientific) with primers (Integrated DNA) for regions within the *AR* promoter and 5'UTR. (Supplementary Table S4). Data was normalized to 2% input. Controls included IgG and Histone3 supplied with the kit.

Statistical analysis.

All results are from at least three independent experiments. Student's t-test was used to compare two groups, while one-way analysis of variance (ANOVA) for comparing more than two groups. Graphs and statistics were generated using GraphPad Prism 9.0.2. A *p*-value less than 0.05 was considered statistically significant. Data met the assumptive criteria of normal distribution and variance.

RESULTS

Tumor-secreted factors TNFα and TGFβ1 suppress stromal AR expression.

To identify tumor-secreted factors that influence stromal AR expression, cytokine array profiling of two prostate cancer cell lines, C4–2, and 22Rv1, was used to identify secreted proteins shared by both cell lines (Fig. 1A; Supplementary Table S5). Treatment of normal BHPrS1 prostate fibroblasts with either TNFα or TGFβ1 for 24h resulted in suppression of *AR* mRNA and protein (Fig. 1B–F). Addition of 10nM synthetic androgen R1881 increased the level of AR protein (Fig. 1E), but not *AR* mRNA (Fig. 1F), consistent with the known role of androgen in stabilizing AR protein [64–66]. However, R1881 did not block the ability of TNFα or TGFβ1 to suppress *AR* mRNA or reduce AR protein (Fig. 1B,E,F). TGFβ1 treatment led to increased expression of CAF markers Col1A1 and αSMA, as well as morphological changes (not shown), as expected [31, 67, 68]; however, TNFα did not cause CAF conversion (Fig. 1D,E). Thus, the loss in AR expression by TNFα is not strictly due to CAF conversion. Three additional tested cytokines, GDF15, FGF9, and bFGF, were unable to suppress AR expression (not shown). These data suggest TNFα may specifically suppress AR expression in prostate stroma fibroblasts through transcriptional repression independent of CAF conversion.

TNFα activates TAK1, NF-κB, and MAPK (p38 and JNK) pathways.

Both TNFα and TGFβ1 downregulate AR expression equally and are not additive when used in combination (Fig. 1F), suggesting they share a common signaling pathway. Both are known to activate TAK1 leading to NF-κB and Jnk/p38 MAPK signaling [69–71]. Since TGFβ1 is a major driver of CAF conversion and TNFα induces AR loss in the absence of CAF conversion, we focused on TNFα. BHPrS1 fibroblasts were treated with TNFα for different times, from 10m to 24h, and activation of NF-κB, TAK1, p38, and Jnk signaling measured. Maximal down-regulation of AR was seen between 18h and 24h (Fig. 2A), which mirrored the activation kinetics of TAK1 (Fig. 2B) strongly suggesting a connection to AR suppression. Within 10min, TNFα rapidly increased IκB phosphorylation, resulting in subsequent IκB degradation, phosphorylation of NF-κB (Fig. 2A), and nuclear translocation (Supplementary Fig. S1A). A similar rapid activation of p38-MAPK and Jnk signaling was also observed (Fig. 2B), although a basal level of p38α activation and nuclear localization

Author Manuscript Author Manuscript Author Manuscript Author Manuscript

was detected (Supplementary Fig. S1B). Activation of all these pathways was sustained through 24h. The p38 target, pCREB/pATF1 is constitutively phosphorylated (Fig. 2C).

TAK1 is not required for TNFα-mediated suppression of AR expression.

To determine if TNFα-mediated inhibition of AR is TAK1 dependent, stromal fibroblasts were treated with two TAK1 inhibitors, 5Z-7 or Takinib [72, 73]. Treatment with 5Z-7 robustly inhibited the downstream pathways, NF-κB, p38α, and Jnk, and rescued TNFα-induced inhibition of *AR* mRNA and protein (Supplementary Fig. S2A,B). However, Takinib only partially rescued AR expression, and had no effect on downstream pathways (Supplementary Fig. S2C). TAK1 expression was silenced with two different siRNAs. Efficient suppression of TAK1 expression failed to rescue AR expression (Supplementary Fig. S2D). Thus, TAK1 is not required for TNFα-mediated suppression of AR and is not required for TNFα-induction of NF-κB, p38, or Jnk. The apparent rescue by 5Z-7 is likely due to non-specific effects on other kinases [72, 73].

Inhibition of NF-κB reverses TNFα-induced AR suppression.

To determine whether NF-κB contributes to TNFα-mediated AR suppression, independent of TAK1, two different NF-κB inhibitors were used to suppress NF-κB signaling. BAY118012 blocks IκB phosphorylation [74], and CAPE blocks NF-κB nuclear translocation [75] (Supplementary Fig S1A). Both prevented TNFα-induced suppression of *AR* mRNA and protein (Fig. 2D,E). Similarly, doxycycline induced expression p65-RelA shRNA blocked TNFα-induced down-regulation of *AR* mRNA and protein (Fig. 2F,G). This occurred in the absence or presence of R1881. Thus, TNFα-induced loss of AR expression in prostate stromal fibroblasts is mediated primarily through NF-κB activation.

p38-MAPK represses basal AR expression.

To determine if MAPK signaling through p38 or Jnk is required for TNFα induced AR downregulation, p38 or Jnk signaling was inhibited. Inhibition of Jnk signaling with two different pan Jnk inhibitors did not rescue AR expression suppressed by TNFα (Supplementary Fig. S3). Treatment of prostate stromal cells with two different pan p38 inhibitors, BIRB796 and SB202190, rescued *AR* mRNA and protein expression suppressed by TNFα (Fig. 3A–C). In fact, the amount of *AR* mRNA and protein in the p38 inhibitor-treated cells was greater than that seen in the control cells. To investigate a possible role for p38, in the suppression of AR expression, independent of TNFα, the p38α isoform was silenced with siRNA in the absence of TNFα. Silencing p38α expression alone, with or without androgen stimulation, resulted in increased expression of *AR* mRNA (Fig. 3D). This indicates p38α plays a suppressive role, independent of androgen, to limit basal levels of AR expression in prostate stromal fibroblasts.

To further determine the role of p38α in the TNFα-mediated suppression of AR, two different siRNAs were used to silence p38α. However, efficient knockdown of p38α was not sufficient to rescue AR protein expression suppressed by TNFα (Fig. 3E). Prior studies demonstrated that other isoforms of p38, especially p38δ, are upregulated when p38α expression is inhibited [76]. Analysis of p38δ mRNA following p38α knockdown revealed a 1.5-fold increase in p38δ mRNA expression (Fig. 3F). To determine the extent to which

Author Manuscript Author Manuscript Author Manuscript Author Manuscript

p38α and/or p38δ contribute to AR downregulation by TNFα, p38α or p38δ alone or in combination were silenced with siRNA. Like p38α knockdown, loss of p38δ also led to an increase in basal AR levels, but still was not sufficient to rescue AR loss induced by TNFα (Fig. 3H). Furthermore, combined loss of both p38α/p38δ also failed to prevent *AR* mRNA and protein downregulation induced by TNFα (Fig. 3G,H). Overall, these findings demonstrate p38α and p38δ are negative regulators of basal levels of AR expression, but they are not involved in TNFα-induced AR suppression.

NF-κB binding regions in the *AR* promoter are required for AR suppression.

The *AR* promoter contains several classical p65/RelA binding sites, some of which have been reported to suppress or enhance AR expression depending on the context [57, 59–61]. In addition, the *AR* promoter contains several predicted CREB/ATF binding sites, classical p38-MAPK targets. To Identify key repressive *AR* regulatory regions, a set of luciferase reporters containing N- and C-terminal deletions in 1.5kb of the *AR* promoter were generated (Fig. 4A). After transient co-transfection with a firefly control plasmid, the ability of TNFα to suppress luciferase reporter activity was measured in WT and mutant reporter transfected cells. Treatment of cells with TNFα resulted in the suppression of luciferase activity on the WT promoter. However, TNFα was no longer able to suppress luciferase activity from mutants harboring deletions from −1040 to −300 (DM1) and from +140 to +300 (DM3) (Fig. 4B). In fact, significantly higher basal levels of luciferase activity were seen in DM1 relative to WT control.

In DM3, one known repressive NF-κB/B-Myb binding site, +142 to +182, one putative NF-κB site, +276 to +285, and one putative C site, +232 to +244 were removed (Fig. 4C). Loss of these elements completely blocked TNFα-induced suppression but did not lead to higher basal levels of expression, consistent with this being a primary region repressed by TNFα via NF-κB signaling. Shorter deletions 3’ to this region did not rescue AR expression (DM4, DM5). In DM1, removal of 5 putative ATF binding sites (−491 to −484; −563 -to −556; −873 to −862; −978 to −967; −1004 to −997) and 4 putative NF-κB sites (−1026 to −1015; −910 to −899; −604 to −595; −426 to −415) (Fig. 4C), completely rescued TNFα-induced suppression and increased basal expression (Fig. 4B), indicating a site within this region that is both basally repressive and sensitive to TNFα signaling. However, further 3’ deletion to −153 (DM4), restored TNFα suppression. This could be due to the inadvertent development of a new cryptic repressive site, or interactions between this 150bp region and the 5’UTR repressive region that mask its repressive activity.

ChIP was used to determine if NF-κB or phosphorylated CREB1/ATF1 bind to any of the predicted promoter elements in *AR* (Fig. 4C). NF-κB was inducibly bound to 2 sites in the *AR* 5’UTR and 3 sites in the *AR* promoter (Fig. 4D). In addition, phosphorylated CREB1/ATF1 was inducibly bound to one site in the 5’UTR. However, no phosphorylated CREB1/ATF1 was found bound to any of the 5 promoter regions in the *AR* promoter (not shown). Thus, TNFα primarily induces NF-κB binding to distinct regions within the AR promoter and 5’UTR. Activated phosphorylated CREB1/ATF1 at the AR 5’UTRmay also contribute to TNFα-mediated AR repression. However, phosphorylated CREB1/ATF1 were not bound within the AR promoter regions that confer repression via p38α/δ.

Author Manuscript Author Manuscript Author Manuscript Author Manuscript

AR suppression in primary patient stromal cells by TNFα, TGFβ, and p38.

To determine if TNFα or TGFβ can suppress AR in patient primary stroma, stromal cells from normal prostate tissue of three different patients were isolated and cultured *in vitro* using established methods [77]. When stromal cultures were treated with TNFα in the presence or absence of R1881, we saw a decrease in AR expression in two of three patients; however, this was reversed by androgen treatment (Fig. 5A,B,C). When the same three stromal cultures were treated with TGFβ1 in the presence or absence of R1881, AR protein was reduced in the presence or absence of androgen (Fig. 5A,B,C), even though androgen increased total AR expression. In three primary lines examined, the levels of p38α induction by TNFα were minimal, as similarly seen in the BHP cells (Fig. 5,B,C,D). To determine if p38 signaling contributes to AR downregulation, p38 was inhibited with BIRB796. Inhibition of p38 with two different concentrations of BIRB796 rescued the AR protein and mRNA expression suppressed by TNFα (Fig. 5D,E). In fact, the amounts of *AR* mRNA and AR protein in the p38 inhibitor-treated cells were greater than those seen in the control cells; as also seen in the BHP cells. We further demonstrated that TNFα, but not TGFβ, induces NF-κB phosphorylation in both BHP and primary cells (Fig. 5C). Thus, TGFβ likely suppresses AR expression through a mechanism that does not involve NF-κB or p38.

Conditioned medium (CM) was used to determine if it is TNFα, or something else, secreted from tumor cells that suppresses AR. BHPrS1 and primary stromal cells were treated for 24 hours with CM collected from 22Rv1 tumor cells after 1 week in culture. 22Rv1-CM was sufficient to suppress AR expression in BHP cells, but not primary cells (Fig. 5F). However, no NF-κB signaling was detected in the CM-treated BHP cells. Furthermore, the primary cells, which are not responsive to TNFα but do respond to TGFβ (Fig. 5B), did not respond to CM. These data suggest that multiple factors may be involved in suppressing stromal AR expression depending on the context.

TNFα and p38-MAPK negatively control stromal AR target genes.

To determine what factors are secreted by the prostate stromal fibroblasts in response to androgen stimulation, qRT-PCR was used to interrogate known prostate morphogens. Treatment of stromal cells with R1881, increased the levels of *FGF10* and *WNT16* mRNA 4-fold, but not *FGF7* mRNA (Fig. 6A). Based on immunoblotting, R1881 led to a clear induction of FGF10 protein and a modest induction of Wnt16 (Fig. 6B). Due to their hydrophobic nature, secreted Wnts are difficult to detect by standard ELISA [91]. To better measure Wnt16 production by androgen, prostate stromal fibroblasts were treated with the porcupine inhibitor, IWP-2, to block Wnt secretion, which led to increased accumulation of Wnt16 within the cell (Fig. 6C). IWP-2-induced accumulation of Wnt16 in the cell was further enhanced by R1881 treatment (Fig. 6C), indicating androgen enhances Wnt16 levels.

When stromal fibroblasts were treated with TNFα in the presence of R1881, AR targets *FGF10* and *WNT16*, but not *FGF7*, were downregulated (Fig. 6D). Conversely, when p38α was knocked down by siRNA, both *FGF10* and *WNT16* mRNA were increased ~3-fold, and this was dramatically enhanced up to 10-fold upon stimulation with androgen (Fig. 6E). *FGF7* mRNA was not repressed by TNFα but instead enhanced ~2-fold (Fig. 6D).

Author Manuscript Author Manuscript Author Manuscript Author Manuscript

FGF7 mRNA was increased 3.5-fold by loss of p38α, but this was not further enhanced by androgen treatment (Fig. 6E). Altogether, these findings indicate that FGF10 and Wnt16, but not FGF7(KGF), are classical targets induced by androgen in prostate stromal cells; their expression is influenced by TNFα, NF-κB, and p38α, which also control AR expression.

Wnt16 maintains prostate basal cell survival via Jnk signaling.

Numerous studies have shown the primary function of FGF10 is to suppress epithelial proliferation and drive luminal cell differentiation [2, 8, 12, 16, 21, 63, 78]. To determine how Wnt16 contributes to epithelial cell homeostasis, PrEC cells were treated with Wnt16 and the effects on canonical and non-canonical signaling measured. Treatment with Wnt16 had no effect on β-catenin nuclear localization or its phosphorylation, but instead lead to a dramatic increase in Jnk signaling (Fig. 7A,B). Treatment of PrECs with two different Jnk inhibitors resulted in loss of Jnk signaling (Fig. 7C) and significant loss of PrEC viability (Fig. 7D; Supplementary Fig. S4), and loss of both basal and Wnt-induced Jnk signaling (Fig. 7E). Thus, Wnt16 contributes to epithelial homeostasis via non-canonical signaling to maintain basal cell survival.

DISCUSSION

The findings from this study provide new insights into possible molecular mechanisms underlying the regulation of AR expression in prostate stromal fibroblasts and has many implications for prostate cancer etiology. We identified at least two tumor-secreted factors, TNFα and TGFβ1, which could play a role in suppressing stromal fibroblast AR expression. Mechanistically, loss of AR expression occurs through transcriptional repression at the *AR* promoter. Specifically, TNFα mediates repression of *AR* expression through classical NF-κB/RelA signaling, independent of CAF conversion, by acting at two regions encompassing 5 binding sites within the *AR* promoter, −1000 to −300bp upstream and within the 5'-UTR. CREB1/ATF1 was also found to be activated within the 5'-UTR. Another unexpected mechanistic finding is that p38α and p38δ are negative regulators of basal AR expression. Suppression of *AR* by p38-MAPK is localized −1000 to −300bp upstream of the *AR* transcriptional initiation site. However, activated CREB1/ATF1 is not likely responsible for this repression. While these studies strongly support a transcriptional repressive mechanism, we cannot rule out the possibility there are additional mechanisms involved through regulation of mRNA or protein stability.

This is the first study to investigate the mechanisms of *AR* promoter repression in a normal human cell type. Most human *AR* promoter studies have been conducted in metastatic tumor cell lines where promoter dysregulation is a major mechanism driving prostate cancer progression. A few *AR* promoter studies have been conducted in normal tissues of rats, where there are distinct species differences [41]. In rat Sertoli cells, TNFα/TGFβ1 were shown to enhance AR expression [60]. However, NF-κB repressed AR expression in human tumor cells via the negative regulatory element within the 5'-UTR of the *AR* gene, through a RelA/Myb repressor complex [61]. Our studies suggest this same NF-κB repressive element, as well as one 100bp further downstream and close to a CREB1/ATF1 binding site may also be important for TNFα-mediated repression of *AR* in human prostate fibroblasts. Our

Author Manuscript Author Manuscript Author Manuscript Author Manuscript

studies also identified a second TNFα-repressive region at −1000 to −300, where three TNFα-induced binding sites for NF-κB were identified.

The effects of TNFα or TGFβ1 on AR suppression were further validated in freshly isolated primary stromal cells. TGFβ1 significantly suppressed AR expression in three isolates, whereas TNFα only modestly repressed in two isolates. This discrepancy could be due to heterogeneity of the isolates, being made up of both smooth muscle and fibroblasts, and/or relative levels of respective receptor expression. TNFα also induced NF-κB signaling in primary cells, similarly to the immortalized cells, but TGFβ did not. Interestingly, blocking p38-MAPK signaling led to elevated AR expression, just as we observed in our immortalized cell line, strongly supporting the new finding that p38-MAPK signaling acts as a suppressor of AR expression in prostate stroma.

The biological implications of AR loss in the stroma are highlighted by the fact that loss of AR expression, either through TNFα or p38-MAPK signaling, leads to loss of two stromal AR target morphogens, FGF10 and Wnt16, but not FGF7 (aka KGF). FGF10 and FGF7 are known morphogens for prostate organogenesis, which act on the basal cells to initiate luminal cell differentiation [12, 13, 19, 21, 22, 79]. That FGF10 is an AR target is well-documented, but FGF7 doesn't seem to be a strong candidate for an AR target in fibroblasts [14, 17, 18, 78]. However, one report suggests the source of AR-induced FGF10 might be different from that of FGF7, i.e., one from fibroblasts and the other from smooth muscle. This would be consistent with mouse genetic studies where loss of AR in both cell types is more severe than either cell type alone [4, 5, 80]. It was first observed in the WPMY fibroblast cell line that overexpression of AR was sufficient to increase *WNT16* mRNA expression [81]. In the BHPrS1 line, we found that just adding androgen was sufficient to induce *WNT16* mRNA. Both *FGF10* and *WNT16* are super activated by androgen when p38α/δ signaling is blocked, further confirming these are true targets of androgen signaling via AR in prostate fibroblasts. We have not yet determined whether they are direct or indirect AR targets.

We extended these studies to demonstrate that Wnt16 acts on basal prostate epithelial cells to sustain their survival through non-canonical Jnk signaling. Luminal cell adhesion to the basal cell layer via E-cadherin is critical for maintaining luminal cell survival in the normal gland [21], hence, loss of basal cells in the normal gland would disrupt homeostasis. Loss of basal cells is in fact a hallmark of high grade PIN in prostate cancer [82], where presumably intrinsic luminal AR or other pathways drive tumor cell survival. The mechanisms that lead to basal cell loss are unknown, but our studies strongly suggest that Wnt16 secretion is lost upon stromal AR loss, leading to basal cell death and their loss during oncogenesis.

Identification of NF-κB and p38 signaling as suppressors of AR expression in prostate tumor stroma opens the possibility of using these as biomarkers for prostate cancer aggressiveness, or in co-targeted therapies to restore AR signaling in the stroma. While we identified two possible tumor-secreted factors that can cause stromal AR loss, it seems that neither may be the dominant factor secreted by 22Rv1 cells that mediates this effect. Given there are multiple factors secreted by any one tumor, there are likely multiple ways to suppress stromal AR. The extent to which they cooperate, dominate, or negatively impact

Author Manuscript Author Manuscript Author Manuscript Author Manuscript

each other still needs to be determined. Moreover, it is likely there are differences between patients. In addition, other cells within the tumor microenvironment could be a source for TNFα or TGFβ to suppress stromal AR.

Supplementary Material

Refer to Web version on PubMed Central for supplementary material.

ACKNOWLEDGEMENTS

We thank Carol Kepler in the Tissue Acquisition and Cellular Molecular Analysis Shared Resource (TACMASR) for helping to secure primary prostate stromal cells, Dr. Sander Frank for his cloning expertise, and Dr. Ghassan Mouneimne for critical editing. ST, NS, BC, LJ, YZ, and CKM were supported by funding from NIH/NCI MPI R01 CA254200 and TACMASR by P30 CA023075. ST was additionally supported by funding from NIH/NCI T32 CA009213.

DATA AVAILABILITY

Data sharing is not applicable to this article as no datasets were generated or analyzed during the current study.

REFERENCES

1. Cunha GR. Growth factors as mediators of androgen action during male urogenital development. Prostate Suppl 1996; 6: 22–25. [PubMed: 8630224]
2. Lu W, Luo Y, Kan M, McKeehan WL. Fibroblast growth factor-10. A second candidate stromal to epithelial cell andromedin in prostate. J Biol Chem 1999; 274: 12827–12834. [PubMed: 10212269]
3. Yeh S, Tsai MY, Xu Q, Mu XM, Lardy H, Huang KE et al. Generation and characterization of androgen receptor knockout (ARKO) mice: an in vivo model for the study of androgen functions in selective tissues. Proc Natl Acad Sci U S A 2002; 99: 13498–13503. [PubMed: 12370412]
4. Yu S, Yeh CR, Niu Y, Chang HC, Tsai YC, Moses HL et al. Altered prostate epithelial development in mice lacking the androgen receptor in stromal fibroblasts. Prostate 2012; 72: 437–449. [PubMed: 21739465]
5. Yu S, Zhang C, Lin CC, Niu Y, Lai KP, Chang HC et al. Altered prostate epithelial development and IGF-1 signal in mice lacking the androgen receptor in stromal smooth muscle cells. Prostate 2011; 71: 517–524. [PubMed: 20945497]
6. Hahn AW, Siddiqui BA, Leo J, Dondossola E, Basham KJ, Miranti CK et al. Cancer cell-extrinsic roles for the androgen receptor in prostate cancer. Endocrinology 2023; 164.
7. Cunha GR. Mesenchymal-epithelial interactions: past, present, and future. Differentiation 2008; 76: 578–586. [PubMed: 18557761]
8. Jiang L, Ivich F, Tahsin S, Tran M, Frank SB, Miranti CK et al. Human stroma and epithelium co-culture in a microfluidic model of a human prostate gland. Biomicrofluidics 2019; 13: 064116. [PubMed: 31768202]
9. Hayward SW, Haughney PC, Rosen MA, Greulich KM, Weier HU, Dahiya R et al. Interactions between adult human prostatic epithelium and rat urogenital sinus mesenchyme in a tissue recombination model. Differentiation 1998; 63: 131–140. [PubMed: 9697307]
10. Toivanen R, Shen MM. Prostate organogenesis: tissue induction, hormonal regulation and cell type specification. Development 2017; 144: 1382–1398. [PubMed: 28400434]
11. Thomson AA. Role of androgens and fibroblast growth factors in prostatic development. REPRODUCTION-CAMBRIDGE- 2001; 121: 187–195.
12. Pu Y, Huang L, Birch L, Prins GS. Androgen regulation of prostate morphoregulatory gene expression: Fgf10-dependent and -independent pathways. Endocrinology 2007; 148: 1697–1706. [PubMed: 17218409]

Author Manuscript Author Manuscript Author Manuscript Author Manuscript

13. Yan G, Fukabori Y, Nikolaropoulos S, Wang F, McKeehan WL. Heparin-binding keratinocyte growth factor is a candidate stromal-to-epithelial-cell andromedin. Mol Endocrinol 1992; 6: 2123–2128. [PubMed: 1491693]
14. Planz B, Wang Q, Kirley SD, Lin CW, McDougal WS. Androgen responsiveness of stromal cells of the human prostate: regulation of cell proliferation and keratinocyte growth factor by androgen. J Urol 1998; 160: 1850–1855. [PubMed: 9783973]
15. Nakano K, Fukabori Y, Itoh N, Lu W, Kan M, McKeehan WL et al. Androgen-stimulated human prostate epithelial growth mediated by stromal-derived fibroblast growth factor-10. Endocr J 1999; 46: 405–413. [PubMed: 10503993]
16. Huang L, Pu Y, Alam S, Birch L, Prins GS. The role of Fgf10 signaling in branching morphogenesis and gene expression of the rat prostate gland: lobe-specific suppression by neonatal estrogens. Developmental Biology 2005; 278: 396–414. [PubMed: 15680359]
17. Fasciana C, van der Made AC, Faber PW, Trapman J. Androgen regulation of the rat keratinocyte growth factor (KGF/FGF7) promoter. Biochem Biophys Res Commun 1996; 220: 858–863. [PubMed: 8607856]
18. Nemeth JA, Zelner DJ, Lang S, Lee C. Keratinocyte growth factor in the rat ventral prostate: androgen-independent expression. J Endocrinol 1998; 156: 115–125. [PubMed: 9496241]
19. Thomson AA, Cunha GR. Prostatic growth and development are regulated by FGF10. Development 1999; 126: 3693–3701. [PubMed: 10409514]
20. Ropiquet F, Giri D, Kwabi-Addo B, Schmidt K, Ittmann M. FGF-10 is expressed at low levels in the human prostate. Prostate 2000; 44: 334–338. [PubMed: 10951499]
21. Lamb LE, Knudsen BS, Miranti CK. E-cadherin-mediated survival of androgen-receptor-expressing secretory prostate epithelial cells derived from a stratified in vitro differentiation model. J Cell Sci 2010; 123: 266–276. [PubMed: 20048343]
22. Heer R, Collins AT, Robson CN, Shenton BK, Leung HY. KGF suppresses α2β1 integrin function and promotes differentiation of the transient amplifying population in human prostatic epithelium. J Cell Sci 2006; 119: 1416–1424. [PubMed: 16554439]
23. Frank SB, Miranti CK. Disruption of prostate epithelial differentiation pathways and prostate cancer development. Front Oncol 2013; 3: 273. [PubMed: 24199173]
24. Frank SB, Berger PL, Ljungman M, Miranti CK. Human prostate luminal cell differentiation requires NOTCH3 induction by p38-MAPK and MYC. J Cell Sci 2017; 130: 1952–1964. [PubMed: 28446540]
25. Henshall SM, Quinn DI, Lee CS, Head DR, Golovsky D, Brenner PC et al. Altered expression of androgen receptor in the malignant epithelium and adjacent stroma is associated with early relapse in prostate cancer. Cancer Res 2001; 61: 423–427. [PubMed: 11212224]
26. Wikstrom P, Marusic J, Stattin P, Bergh A. Low stroma androgen receptor level in normal and tumor prostate tissue is related to poor outcome in prostate cancer patients. Prostate 2009; 69: 799–809. [PubMed: 19189305]
27. Leach DA, Need EF, Toivanen R, Trotta AP, Palethorpe HM, Tamblyn DJ et al. Stromal androgen receptor regulates the composition of the microenvironment to influence prostate cancer outcome. Oncotarget 2015; 6: 16135–16150. [PubMed: 25965833]
28. Palethorpe HM, Leach DA, Need EF, Drew PA, Smith E. Myofibroblast androgen receptor expression determines cell survival in co-cultures of myofibroblasts and prostate cancer cells in vitro. Oncotarget 2018; 9: 19100–19114. [PubMed: 29721186]
29. Tang Q, Cheng B, Dai R, Wang R. The role of qndrogen receptor in cross talk between stromal cells and prostate cancer epithelial cells. Front Cell Dev Biol 2021; 9: 729498. [PubMed: 34692685]
30. Liao CP, Chen LY, Luethy A, Kim Y, Kani K, MacLeod AR et al. Androgen receptor in cancer-associated fibroblasts influences stemness in cancer cells. Endocr Relat Cancer 2017; 24: 157–170. [PubMed: 28264911]
31. Caligiuri G, Tuveson DA. Activated fibroblasts in cancer: Perspectives and challenges. Cancer Cell 2023; 41: 434–449. [PubMed: 36917949]

Author Manuscript Author Manuscript Author Manuscript Author Manuscript

32. Tuxhorn JA, Ayala GE, Smith MJ, Smith VC, Dang TD, Rowley DR. Reactive stroma in human prostate cancer: induction of myofibroblast phenotype and extracellular matrix remodeling. Clin Cancer Res 2002; 8: 2912–2923. [PubMed: 12231536]
33. Ishii K, Mizokami A, Tsunoda T, Iguchi K, Kato M, Hori Y et al. Heterogenous induction of carcinoma-associated fibroblast-like differentiation in normal human prostatic fibroblasts by co-culturing with prostate cancer cells. J Cell Biochem 2011; 112: 3604–3611. [PubMed: 21809373]
34. Verona EV, Elkahloun AG, Yang J, Bandyopadhyay A, Yeh IT, Sun LZ. Transforming growth factor-β signaling in prostate stromal cells supports prostate carcinoma growth by up-regulating stromal genes related to tissue remodeling. Cancer Res 2007; 67: 5737–5746. [PubMed: 17575140]
35. Xing F, Saidou J, Watabe K. Cancer associated fibroblasts (CAFs) in tumor microenvironment. Front Biosci (Landmark Ed) 2010; 15: 166–179. [PubMed: 20036813]
36. Kruslin B, Ulamec M, Tomas D. Prostate cancer stroma: an important factor in cancer growth and progression. Bosn J Basic Med Sci 2015; 15: 1–8.
37. Olumi AF, Grossfeld GD, Hayward SW, Carroll PR, Tlsty TD, Cunha GR. Carcinoma-associated fibroblasts direct tumor progression of initiated human prostatic epithelium. Cancer Res 1999; 59: 5002–5011. [PubMed: 10519415]
38. Chen S, Supakar PC, Vellanoweth RL, Song CS, Chatterjee B, Roy AK. Functional role of a conformationally flexible homopurine/homopyrimidine domain of the androgen receptor gene promoter interacting with Sp1 and a pyrimidine single strand DNA-binding protein. Mol Endocrinol 1997; 11: 3–15. [PubMed: 8994183]
39. Faber PW, van Rooij HC, Schipper HJ, Brinkmann AO, Trapman J. Two different, overlapping pathways of transcription initiation are active on the TATA-less human androgen receptor promoter. The role of Sp1. J Biol Chem 1993; 268: 9296–9301. [PubMed: 8486625]
40. Hay CW, Hunter I, MacKenzie A, McEwan IJ. An Sp1 Modulated Regulatory Region Unique to Higher Primates Regulates Human Androgen Receptor Promoter Activity in Prostate Cancer Cells. PLoS One 2015; 10: e0139990. [PubMed: 26448047]
41. Hunter I, Hay CW, Esswein B, Watt K, McEwan IJ. Tissue control of androgen action: The ups and downs of androgen receptor expression. Mol Cell Endocrinol 2018; 465: 27–35. [PubMed: 28789969]
42. Nadiminty N, Tummala R, Lou W, Zhu Y, Zhang J, Chen X et al. MicroRNA let-7c suppresses androgen receptor expression and activity via regulation of Myc expression in prostate cancer cells. J Biol Chem 2012; 287: 1527–1537. [PubMed: 22128178]
43. Grad JM, Dai JL, Wu S, Burnstein KL. Multiple androgen response elements and a Myc consensus site in the androgen receptor (AR) coding region are involved in androgen-mediated up-regulation of AR messenger RNA. Mol Endocrinol 1999; 13: 1896–1911. [PubMed: 10551783]
44. Mizokami A, Yeh SY, Chang C. Identification of 3',5'-cyclic adenosine monophosphate response element and other cis-acting elements in the human androgen receptor gene promoter. Mol Endocrinol 1994; 8: 77–88. [PubMed: 8152432]
45. Yang L, Xie S, Jamaluddin MS, Altuwaijri S, Ni J, Kim E et al. Induction of androgen receptor expression by phosphatidylinositol 3-kinase/Akt downstream substrate, FOXO3a, and their roles in apoptosis of LNCaP prostate cancer cells. J Biol Chem 2005; 280: 33558–33565. [PubMed: 16061480]
46. Shiota M, Yokomizo A, Tada Y, Inokuchi J, Kashiwagi E, Masubuchi D et al. Castration resistance of prostate cancer cells caused by castration-induced oxidative stress through Twist1 and androgen receptor overexpression. Oncogene 2010; 29: 237–250. [PubMed: 19802001]
47. Kang HY, Huang HY, Hsieh CY, Li CF, Shyr CR, Tsai MY et al. Activin A enhances prostate cancer cell migration through activation of androgen receptor and is overexpressed in metastatic prostate cancer. J Bone Miner Res 2009; 24: 1180–1193. [PubMed: 19257827]
48. Yang X, Chen MW, Terry S, Vacherot F, Bemis DL, Capodice J et al. Complex regulation of human androgen receptor expression by Wnt signaling in prostate cancer cells. Oncogene 2006; 25: 3436–3444. [PubMed: 16474850]

Author Manuscript Author Manuscript Author Manuscript Author Manuscript

49. Qiao L, Tasian GE, Zhang H, Cao M, Ferretti M, Cunha GR et al. Androgen receptor is overexpressed in boys with severe hypospadias, and ZEB1 regulates androgen receptor expression in human foreskin cells. Pediatr Res 2012; 71: 393–398. [PubMed: 22391641]
50. Wu D, Sunkel B, Chen Z, Liu X, Ye Z, Li Q et al. Three-tiered role of the pioneer factor GATA2 in promoting androgen-dependent gene expression in prostate cancer. Nucleic Acids Res 2014; 42: 3607–3622. [PubMed: 24423874]
51. He B, Lanz RB, Fiskus W, Geng C, Yi P, Hartig SM et al. GATA2 facilitates steroid receptor coactivator recruitment to the androgen receptor complex. Proc Natl Acad Sci U S A 2014; 111: 18261–18266. [PubMed: 25489091]
52. Alimirah F, Panchanathan R, Chen J, Zhang X, Ho SM, Choubey D. Expression of androgen receptor is negatively regulated by p53. Neoplasia 2007; 9: 1152–1159. [PubMed: 18084622]
53. Davis JN, Wojno KJ, Daignault S, Hofer MD, Kuefer R, Rubin MA et al. Elevated E2F1 inhibits transcription of the androgen receptor in metastatic hormone-resistant prostate cancer. Cancer Res 2006; 66: 11897–11906. [PubMed: 17178887]
54. Valdez CD, Davis JN, Odeh HM, Layfield TL, Cousineau CS, Berton TR et al. Repression of androgen receptor transcription through the E2F1/DNMT1 axis. PLoS One 2011; 6: e25187. [PubMed: 21966451]
55. Dai JL, Burnstein KL. Two androgen response elements in the androgen receptor coding region are required for cell-specific up-regulation of receptor messenger RNA. Mol Endocrinol 1996; 10: 1582–1594. [PubMed: 8961268]
56. Cai C, He HH, Chen S, Coleman I, Wang H, Fang Z et al. Androgen receptor gene expression in prostate cancer is directly suppressed by the androgen receptor through recruitment of lysine-specific demethylase 1. Cancer Cell 2011; 20: 457–471. [PubMed: 22014572]
57. Zhang L, Altuwaijri S, Deng F, Chen L, Lal P, Bhanot UK et al. NF-κB regulates androgen receptor expression and prostate cancer growth. Am J Pathol 2009; 175: 489–499. [PubMed: 19628766]
58. Zaidi G, Supakar PC. Identification of a nuclear protein interacting with a novel site on rat androgen receptor promoter after transcription factor NFkB is displaced from adjacent site. Mol Biol Rep 2003; 30: 121–125. [PubMed: 12841583]
59. Song CS, Jung MH, Supakar PC, Chen S, Vellanoweth RL, Chatterjee B et al. Regulation of androgen action by receptor gene inhibition. Ann N Y Acad Sci 1995; 761: 97–108. [PubMed: 7625753]
60. Delfino FJ, Boustead JN, Fix C, Walker WH. NF-κB and TNFα stimulate androgen receptor expression in Sertoli cells. Mol Cell Endocrinol 2003; 201: 1–12. [PubMed: 12706288]
61. Ko S, Shi L, Kim S, Song CS, Chatterjee B. Interplay of NF-κB and B-myb in the negative regulation of androgen receptor expression by tumor necrosis factor alpha. Mol Endocrinol 2008; 22: 273–286. [PubMed: 17975021]
62. Hay CW, Watt K, Hunter I, Lavery DN, MacKenzie A, McEwan IJ. Negative regulation of the androgen receptor gene through a primate-specific androgen response element present in the 5' UTR. Horm Cancer 2014; 5: 299–311. [PubMed: 24895212]
63. Berger PL, Frank SB, Schulz VV, Nollet EA, Edick MJ, Holly B et al. Transient induction of ING4 by Myc drives prostate epithelial cell differentiation and its disruption drives prostate tumorigenesis. Cancer Res 2014; 74: 3357–3368. [PubMed: 24762396]
64. Chen S, Xu Y, Yuan X, Bubley GJ, Balk SP. Androgen receptor phosphorylation and stabilization in prostate cancer by cyclin-dependent kinase 1. Proc Natl Acad Sci U S A 2006; 103: 15969–15974. [PubMed: 17043241]
65. Yeap BB, Krueger RG, Leedman PJ. Differential posttranscriptional regulation of androgen receptor gene expression by androgen in prostate and breast cancer cells. Endocrinology 1999; 140: 3282–3291. [PubMed: 10385425]
66. Lee DK, Chang C. Endocrine mechanisms of disease: Expression and degradation of androgen receptor: mechanism and clinical implication. J Clin Endocrinol Metab 2003; 88: 4043–4054. [PubMed: 12970260]

Author Manuscript Author Manuscript Author Manuscript Author Manuscript

67. Lamprecht S, Sigal-Batikoff I, Shany S, Abu-Freha N, Ling E, Delinasios GJ et al. Teaming up for trouble: Cancer cells, transforming growth factor-β1 signaling and the epigenetic corruption of stromal naïve fibroblasts. Cancers (Basel) 2018; 10.
68. Hawinkels LJ, Paauwe M, Verspaget HW, Wiercinska E, van der Zon JM, van der Ploeg K et al. Interaction with colon cancer cells hyperactivates TGF-β signaling in cancer-associated fibroblasts. Oncogene 2014; 33: 97–107. [PubMed: 23208491]
69. Silverman N, Zhou R, Erlich RL, Hunter M, Bernstein E, Schneider D et al. Immune activation of NF-κB and JNK requires Drosophila TAK1. J Biol Chem 2003; 278: 48928–48934. [PubMed: 14519762]
70. Vidal S, Khush RS, Leulier F, Tzou P, Nakamura M, Lemaitre B. Mutations in the Drosophila dTAK1 gene reveal a conserved function for MAPKKKs in the control of rel/NF-kappaB-dependent innate immune responses. Genes Dev 2001; 15: 1900–1912. [PubMed: 11485985]
71. Thiefes A, Wolter S, Mushinski JF, Hoffmann E, Dittrich-Breiholz O, Graue N et al. Simultaneous blockade of NFkappaB, JNK, and p38 MAPK by a kinase-inactive mutant of the protein kinase TAK1 sensitizes cells to apoptosis and affects a distinct spectrum of tumor necrosis factor [corrected] target genes. J Biol Chem 2005; 280: 27728–27741. [PubMed: 15837794]
72. Ninomiya-Tsuji J, Kajino T, Ono K, Ohtomo T, Matsumoto M, Shiina M et al. A resorcylic acid lactone, 5Z-7-oxozeaenol, prevents inflammation by inhibiting the catalytic activity of TAK1 MAPK kinase kinase. J Biol Chem 2003; 278: 18485–18490. [PubMed: 12624112]
73. Zimmerman EI, Gibson AA, Hu S, Vasilyeva A, Orwick SJ, Du G et al. Multikinase inhibitors induce cutaneous toxicity through OAT6-mediated uptake and MAP3K7-driven cell death. Cancer Res 2016; 76: 117–126. [PubMed: 26677977]
74. Monteiro C, Miarka L, Perea-García M, Priego N, García-Gómez P, Álvaro-Espinosa L et al. Stratification of radiosensitive brain metastases based on an actionable S100A9/RAGE resistance mechanism. Nat Med 2022; 28: 752–765. [PubMed: 35411077]
75. Zhang X, Zheng S, Hu C, Li G, Lin H, Xia R et al. Cancer-associated fibroblast-induced lncRNA UPK1A-AS1 confers platinum resistance in pancreatic cancer via efficient double-strand break repair. Oncogene 2022; 41: 2372–2389. [PubMed: 35264742]
76. Wang H, Xu Q, Xiao F, Jiang Y, Wu Z. Involvement of the p38 mitogen-activated protein kinase α, β, and γ isoforms in myogenic differentiation. Mol Biol Cell 2008; 19: 1519–1528. [PubMed: 18256287]
77. Richards Z, McCray T, Marsili J, Zenner ML, Manlucu JT, Garcia J et al. Prostate stroma increases the viability and maintains the branching phenotype of human prostate organoids. iScience 2019; 12: 304–317. [PubMed: 30735898]
78. Watson J, Francavilla C. Regulation of FGF10 signaling in development and disease. Front Genet 2018; 9: 500. [PubMed: 30405705]
79. Madueke IC, Hu WY, Huang L, Prins GS. WNT2 is necessary for normal prostate gland cyto-differentiation and modulates prostate growth in an FGF10 dependent manner. Am J Clin Exp Urol 2018; 6: 154–163. [PubMed: 30246051]
80. Lai KP, Yamashita S, Vitkus S, Shyr CR, Yeh S, Chang C. Suppressed prostate epithelial development with impaired branching morphogenesis in mice lacking stromal fibromuscular androgen receptor. Mol Endocrinol 2012; 26: 52–66. [PubMed: 22135068]
81. Tanner MJ, Welliver RC Jr., Chen M, Shtutman M, Godoy A, Smith G et al. Effects of androgen receptor and androgen on gene expression in prostate stromal fibroblasts and paracrine signaling to prostate cancer cells. PLoS One 2011; 6: e16027. [PubMed: 21267466]
82. Bostwick DG. Prostatic intraepithelial neoplasia (PIN): current concepts. J Cell Biochem Suppl 1992; 16h: 10–19. [PubMed: 1289664]

Author Manuscript Author Manuscript Author Manuscript Author Manuscript

A)

Table 1: Shared Tumor Cytokines

High	Med/Hi	Medium
GDF-15	EGF	BMP4
MIF	FGF6,9	GDNF
PSA	NT3,4	IGFBP3
CCL3,4	VEGFA	CXCL10
BDNF	bFGF	MMP2
TGFβ	IL8	OPN
PDGF-BB	CXCL1	CNTF
CCL5	TNFα	PAI-I
OSM	MMP7	CXCL4

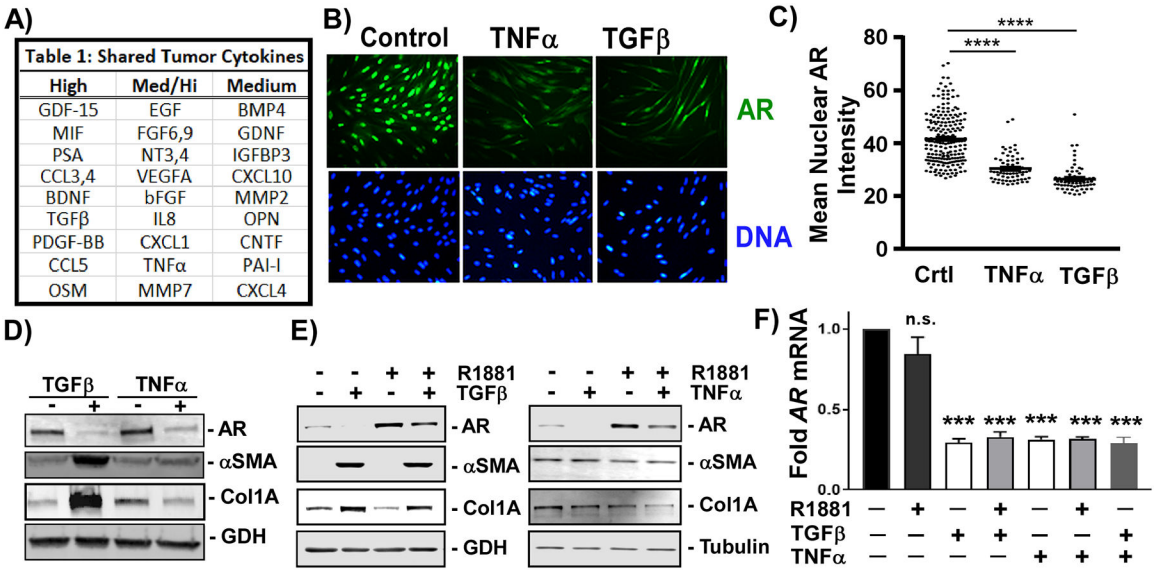

Figure 1: TNFα and TGFβ suppress AR expression.

A) Relative level (high, med/high, and medium) of secreted proteins shared by two prostate cancer cell lines, C4–2 and 22Rv1, based on cytokine array profiling. **B-F)** BHPrS1 cells treated with 30ng/ml TNFα or 10ng/ml TGFβ1 for 24h with or without 10nM R1881. **B)** Immunostaining for AR and nuclear staining with Hoechst (DNA) after R1881 treatment, captured by epifluorescence imaging. **C)** Quantification of nuclear staining in B. n=50, ****p<0.0001. **D,E)** Immunoblotting for AR, αSMA, Col1A1, and GAPDH (GDH) or Tubulin. **F)** Fold change in AR mRNA as measured by qRT-PCR, relative to GAPDH and expressed fold change relative to untreated control. Error bars = SD, n=3, ***p<0.001. n.s. not significant.

Author Manuscript Author Manuscript Author Manuscript Author Manuscript

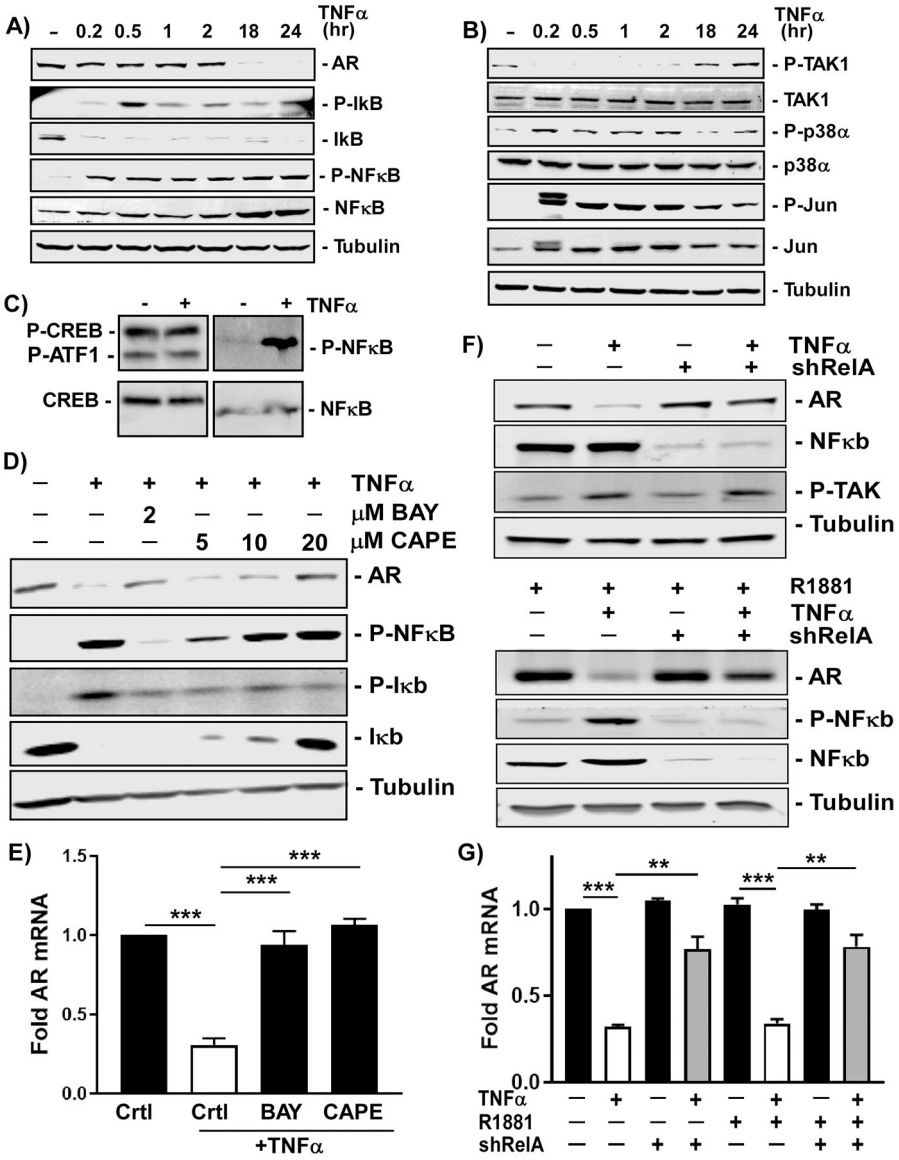

Figure 2: TNFα activates NF-κB to mediate TNFα-induced AR suppression.

A,B) BHPrS1 cells treated with 30ng/ml TNFα for different times from 10m to 24h. Activation of TAK1 (P-TAK1), NFκB (P-NFκB, P-IκB), p38α (P-p38α), and Jnk (P-Jun) measured by immunoblotting. Controls included Tubulin and total levels of TAK1, IκB, NFκB, p38α, and Jun. **C)** BHPrS1 cells treated with 30ng/ml TNFα for 24 hr. Activated CREB1/ATF1 (P-CREB/P-ATF1), NF-κB (P-NFκB), and total levels measured by immunoblotting. **D,E)** BHPrS1 cells treated with 30ng/ml TNFα for 24h w/wo 2μM BAY118012 or different concentrations of CAPE. **D)** Levels of AR, P-NFκB, P-IκB, IκB, and Tubulin assessed by immunoblotting. **E)** Fold change in *AR* mRNA measured by qRT-PCR w/wo 2μM BAY118012 and 20μM CAPE. Error bars = SD, n=3, ***p<0.001. **F,G)** Cells expressing Tet-inducible shRelA treated w/wo 200ng/ml doxycycline for 24h, followed by 30ng/ml TNFα, w/wo 10nM R1881 for 24h. **F)** Level of AR, P-NFκB,

Author Manuscript Author Manuscript Author Manuscript Author Manuscript

P-TAK1, NFκB, and Tubulin measured by immunoblotting. **G)** Fold change in *AR* mRNA measured by qRT-PCR. Error bars = SD, n=3, $^{**}p<0.005$, $^{***}p<0.001$.

Author Manuscript Author Manuscript Author Manuscript Author Manuscript

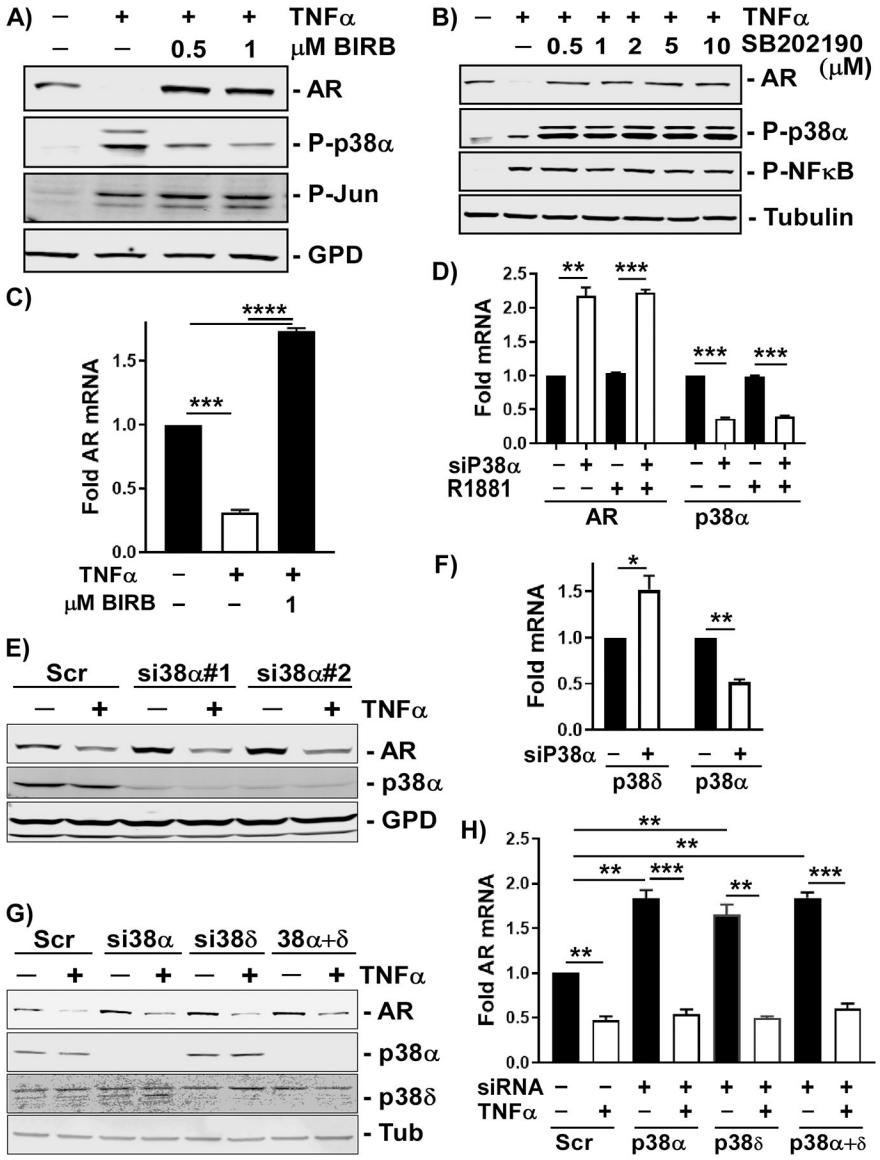

Figure 3: p38-MAPK suppresses basal levels of AR expression.

A,B) BHPrS1 cells treated with 30ng/ml TNFα for 24h w/wo several doses of p38-MAPK inhibitors, BIRB796 and SB202190. Levels of AR, P-p38α, P-Jun, and GAPDH (GDH) assessed by immunoblotting. **C)** BHPrS1 cells treated with 30ng/ml TNFα for 24h w/wo 0.5 μM BIRB796 and fold change in *AR* mRNA measured by qRT-PCR. Error bars = SD, n=3, ***p<0.001; ****p<0.0005. **D)** BHPrs1 cells transfected with scrambled (−) or siRNA to p38α (+) for 24h, then treated w/wo 10nM R1881 for 24h. Fold change in *AR* and p38α mRNA measured by qRT-PCR. Error bars = SD, n=3, **p<0.005, ***p<0.001. **E)** BHPrs1 cells transfected with scrambled or two different siRNAs to p38α (#1, #2) for 24h, then treated with w/wo 30ng/ml TNFα for 24h. Levels of AR, p38α, and tubulin measured by immunoblotting. **F)** BHPrS1 cells transfected with scrambled (−) or siRNA to p38α (+) for 24h. Fold change in p38α and p38δ mRNA measured by qRT-PCR. Error bars = SD, n=5, *p<0.01, **p<0.005. **G, H)** BHPrS1 cells transfected with scrambled, siRNA to p38α,

siRNA to p38δ, or in combination, for 24h, then treated with w/wo 30ng/ml TNFα for 24h. **G)** Levels of AR, p38α, p38δ, and tubulin measured by immunoblotting. **H)** Fold change in *AR* mRNA measured by qRT-PCR. Error bars = SD, n=3, $**p<0.005$; $***p<0.001$.

Author Manuscript Author Manuscript Author Manuscript Author Manuscript

Author Manuscript Author Manuscript Author Manuscript Author Manuscript

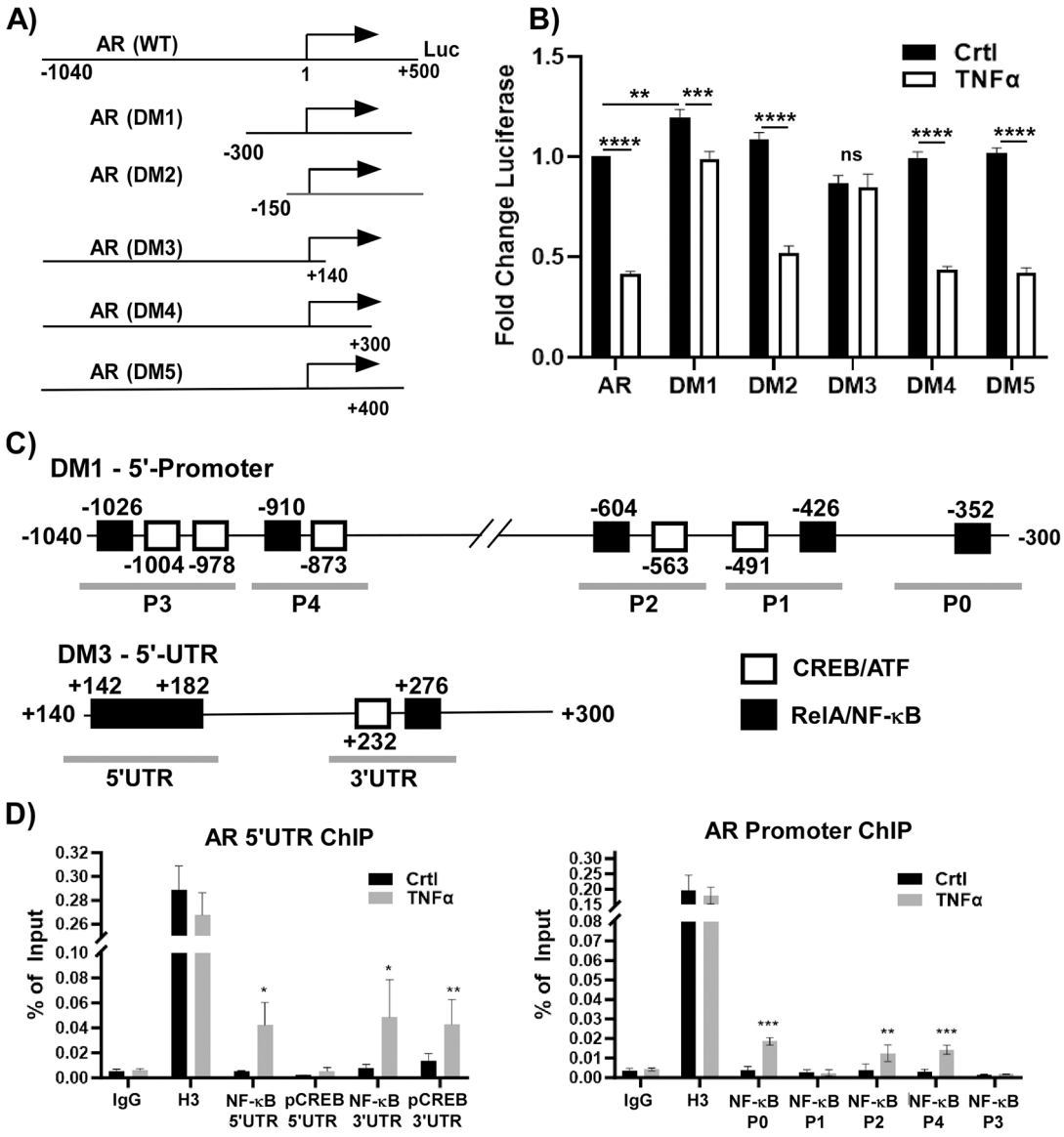

Figure 4: NF-κB and p38-MAPK target RelA and ATF binding regions in the AR promoter to control AR expression.

A) Diagram of wild type *AR* promoter luciferase reporter and deletion mutants. **B)** BHPrS1 cells were transiently transfected with nano luciferase control vector, wild type *AR* promoter, or indicated mutant promoters along with firefly control. Transfected cells were treated w/wo 30ng/ml TNFα for 24h. Levels of nano luciferase activity relative to firefly control were measured. Error bars = SD. n=4, **p<0.005, ***p<0.001; ****p<0.0001. **C)** Predicted CREB/ATF and RelA binding elements in *AR* promoter deletion mutants DM1 and DM3. PCR primer regions for ChIP assay indicated (P0-P4, UTR). **D)** ChIP qPCR quantification, as percentage of input, of NF-κB and phosphorylated CREB/ATF1 binding at indicated sites (**C)**) within the AR promoter and 5'-UTR. Error bars = SD. n=4, *p<0.05, **p<0.01, ***p<.005.

Author Manuscript Author Manuscript Author Manuscript Author Manuscript

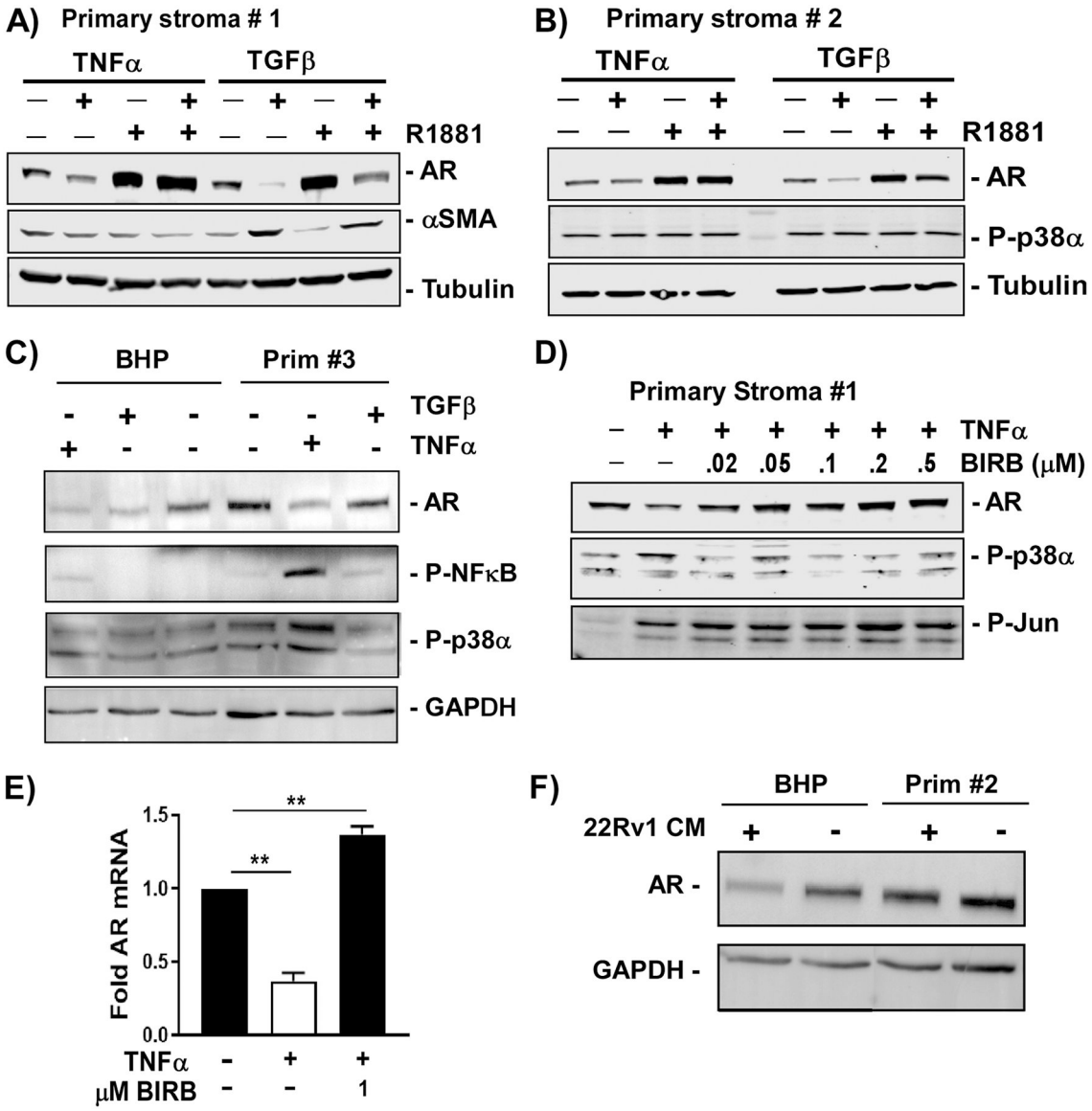

Figure 5: AR suppression in primary stromal cells.

A,B) Primary stroma from different patients treated (#1, #2) treated with 30ng/ml TNFα and TGFβ1 for 24h w/wo R1881. Levels of AR, αSMA, pP38α, pJun, and Tubulin assessed by immunoblotting. **C)** Primary stroma #3 (Prim #3) and BHPrS1 (BHP) cells treated with 30ng/ml TNFα or 10ng/ml TGFβ1 for 24 hr. Levels of AR, activated NF-κB (P-NFκB) and p38α (P-p38α), and GAPDH assessed by immunoblotting. **D,E)** Primary stroma #1 treated several doses of p38-MAPK inhibitors, BIRB796 w/wo 30ng/ml TNFα. **D)** Levels of AR, pP38α, pJun, assessed by immunoblotting. **E)** *AR* mRNA measured by qRT-PCR. Error bars = SD, n=2, $^{**}p<0.001$. **F)** Conditioned medium (CM) was collected from 22Rv1 cells grown in culture for 1 week. Primary stroma #2 (Prim #2) and BHPrS1 (BHP) cells were treated with a 1:1 ratio of CM and fresh growth medium for 24 hours. Levels of AR and GAPDH assessed by immunoblotting.

Author Manuscript Author Manuscript Author Manuscript Author Manuscript

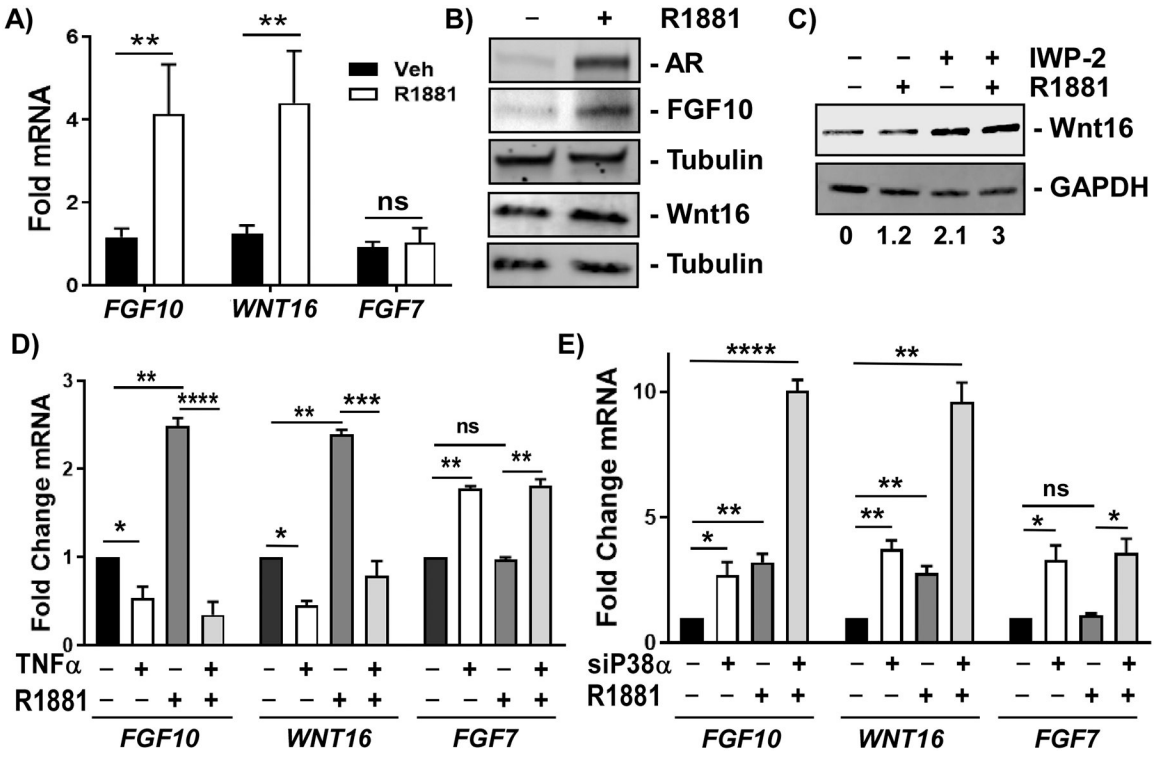

Figure 6: FGF10 and Wnt16 are stromal AR targets suppressed by TNFα and p38-MAPK.

BHPrS1 cells treated w/wo 10nM R1881 for 24h. **A)** Fold change in levels of *FGF10*, *WNT16*, and *FGF7*(KGF) measured by qRT-PCR. Error bars = SD. n=3, $^{**}p<0.005$. **B)** Levels of AR, FGF10, Wnt16, and tubulin following treatment w/wo R1881 assessed by immunoblotting. **C)** Levels of Wnt16 after treatment w/wo 5μM porcupine inhibitor (IWP-2) for 24h w/wo 10nM R1881. **D)** BHPrS1 cells treated with 30ng/ml TNFα for 24 hours w/wo 10nM R1881. Fold change in *FGF7*, *FGF10*, and *WNT16* mRNA measured by qRT-PCR. Error bars = SD. n=3, $^{**}p<0.005$, $^{***}p<0.001$, ****p<0.0001. **E)** BHPrS1 cells transfected with scrambled or siRNA to p38α and treated w/wo 10nM R1881. Fold change in *FGF7*, *FGF10*, and *WNT16* mRNA measured by qRT-PCR. Error bars = SD. n=3, $^{*}p<0.01$, $^{**}p<0.005$, $^{****}p<0.0001$.

Author Manuscript Author Manuscript Author Manuscript Author Manuscript

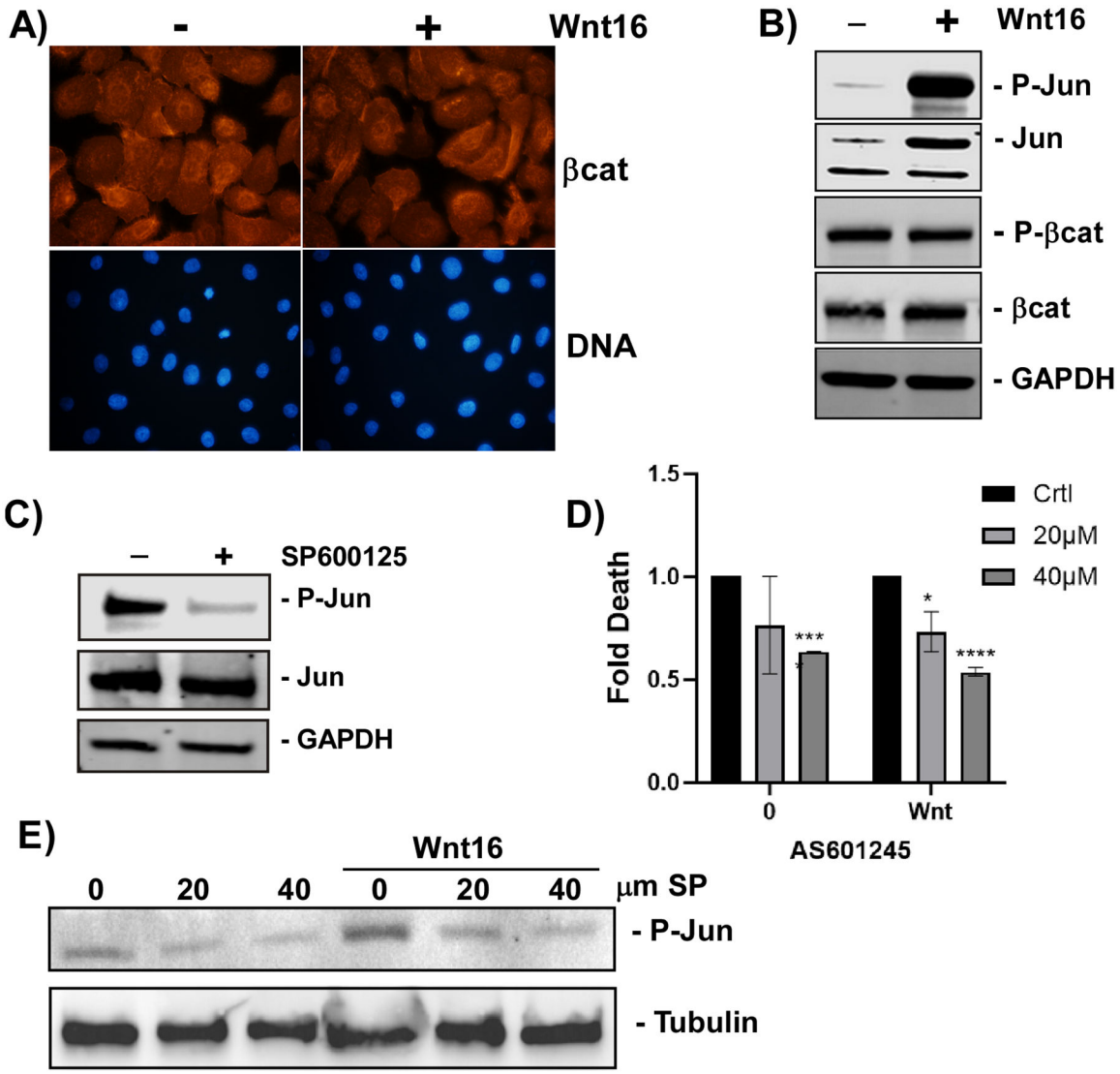

Figure 7: Wnt16 maintains prostate basal cell survival via Jnk signaling.

A,B) PrEC in starvation medium treated with 200ng/ml recombinant Wnt16 for 24h. **A)** Nuclear localization of β-catenin measured by immunostaining. **B)** Activation of β-Catenin (P-βCat), total β-catenin (βCat), and Jnk signaling, P-Jun and total Jun, and GAPDH measured by immunoblotting. **C)** PrEC in growth medium treated with 20μM Jnk inhibitor SP600125 for 24 hr. Levels of activated Jun (P-Jun), total Jun, and GAPDH measured by immunoblotting. **D,E)** PrEC in starvation medium treated w/wo 200ng/ml Wnt16 for 2 hours w/wo different concentrations of **D)** AS601245 or **E)** SP600125. **D)** Viability measured by crystal violet staining. **E)** Level of Jnk activation (P-Jun) and Tubulin measured by immunoblotting.